Published in Applied Physics Letters 72, 404-406, 1998
which should be used for any reference to this work

Loss measurements on semiconductor lasers by Fourier analysis of the emission spectra

Daniel Hofstetter[a] and Robert L. Thornton
Xerox Palo Alto Research Center, Palo Alto, California 94304

We present a study on a novel method for the determination of the cavity losses in semiconductor lasers. The method we use involves Fourier analysis of the Fabry–Pérot mode spectrum when operating the device below lasing threshold. The observation of the decay rate of higher order harmonics in the Fourier analysis of the spectra allows us to determine the amount of cavity propagation loss/gain. A comparison between experimental and calculated data for an AlGaInP laser at 670 nm showed good agreement up to an injection current of $0.93\times I_{\mathrm{th}}$. This method therefore provides a generalization of the Fabry–Pérot contrast measurement method for extracting cavity losses from spectral information.

The characterization of laser cavities in terms of internal loss or gain is a research topic of ongoing relevance and importance, especially with regard to the development of new laser materials and designs in the short wavelength range of the spectrum. An elegant method to determine the losses is based on a measurement of the Fabry–Pérot (FP) fringe contrast, m, in the spectrum.[1–3] The contrast is defined as $m=(I_{\max}-I_{\min})/(I_{\max}+I_{\min})$. This method is very effective for low Q cavities when m is significantly less than 1. As the Q factor of the cavity increases, the modes become more and more like Dirac–delta functions, with the contrast m approaching unity, and a narrow linewidth, whereas the FP modes of a low Q factor cavity exhibit a nearly sinusoidal, low contrast pattern.

In this work, we show a new method to measure the optical gain of semiconductor laser cavities. The detailed analysis of Fourier transformed subthreshold spectra[4,5] allowed us to determine a wavelength-averaged cavity propagation loss/gain. The Fourier transform of the FP fringe pattern results in a spectrum containing the fundamental FP frequency related to the cavity length plus harmonics thereof.[6] As will be shown below, the cavity propagation loss/gain is related to the ratio between the Fourier coefficients of adjacent harmonics. On the other hand, the width of the individual harmonic peaks is also inversely proportional to the spectral bandwidth of the light emission.[7,8] Therefore, by using the propagation loss/gain as a fitting parameter to match theoretically transformed spectra to experimental data, we can obtain a measurement of the internal cavity losses. This method is especially well suited as a diagnostic tool for light emitters which exhibit stimulated emission but are not lasing. It is superior to the FP contrast measurement method[1,2] in the respect that it continues to be useful as m approaches unity and in fact is limited only by the resolution of the spectrometer used. In addition, it potentially allows filtering of TE/TM mode families determining their gain independently; these different mode sets would make the correct determination of the contrast, and therefore the use of the Hakki–Paoli method more difficult. Finally, by using this new technique, the point of zero propagation loss, or transparency current level, can be found easily.

In order to show how well this simple analysis applies to experimental data, we present here spectral measurements of GaInP/AlGaInP-based red diode lasers,[9,10] which will be compared with calculations. The laser material was a conventional red laser structure with 500 nm thick $Al_{0.5}In_{0.5}P$ cladding layers, a 240 nm thick $(Al_{0.6}Ga_{0.4})_{0.5}In_{0.5}P$ waveguide core with an 8 nm thick GaInP quantum well in the center. It was grown on a 10° misoriented GaAs substrate by metalorganic chemical vapor deposition. The emission wavelength of these devices was 670 nm, corresponding to a Ga mole fraction of 0.4 in the alloy composition $Ga_xIn_{1-x}P$ of the quantum well. After deposition of 50 μm wide Ti/Au stripes to form broad area p contacts, and Au/Ge n-contact metallurgy, 450 μm long laser bars were cleaved from the material. These broad area devices were probe tested at room temperature and under pulsed conditions (800 ns pulse length, 0.08% duty cycle). The emitted light was collected by a fiber and fed onto the 50 μm wide slit of a high resolution grating spectrometer (SPEX, 1.26 m focal length, 0.25 Å spectral resolution, $\Lambda=1800$ lines/mm). Light detection was accomplished by a 1024 element array photodetector. Using this configuration, spectral measurements of a 10 nm wavelength range with a theoretical resolution of 0.1 Å could be performed. Due to the pulsed operation of the laser diode, it was necessary to collect the light of the investigated device for up to 30 s.

The analytic expression for a subthreshold diode laser spectrum makes use of the optical transmission spectrum through a FP resonator. The geometrical series expansion of the transmitted amplitude through such a resonator is given by

$$A(\beta)=(1-R\times e^{-2i\psi})\times\sum_{m=0}^{\infty}(R\times e^{2i\psi})^m\times e^{2inmL\beta}\times e^{-2(m+0.5)kL\beta}, \tag{1}$$

where $\beta=2\pi/\lambda$ is the wave number, n represents the refractive index, k corresponds to the absorption index, R is the power reflectance of the laser mirrors, L stands for the cavity length and $\psi=\arctan(-2k/n^2+k^2-1)$ is the phase change of

[a]Electronic mail: hofstetter@parc.xerox.com

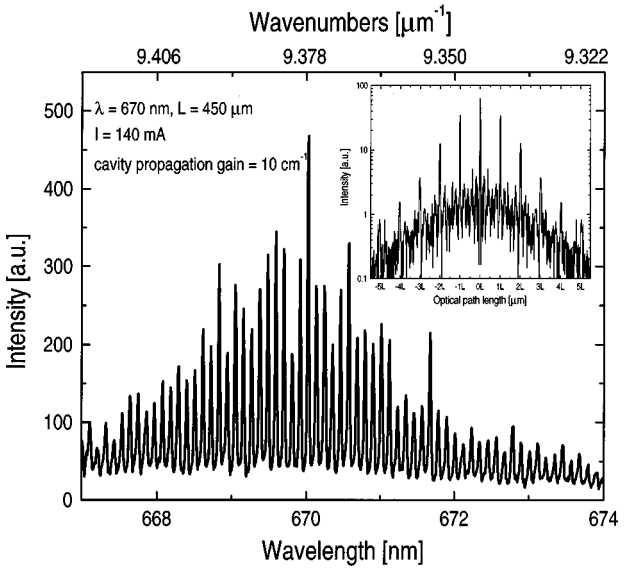

FIG. 1. High resolution laser spectrum of a red laser at $0.933\times I_{\mathrm{th}}$. The inset shows the Fourier transform of this spectrum.

the light due to the facet reflection. The transmitted intensity can then be calculated according to $I(\beta)=A(\beta)\times A^*(\beta)$, and, somewhat simplified, the subthreshold emission spectrum of a diode laser can be described as the product $S(\beta)=I(\beta)\times E(\beta)$ of the transmitted intensity through a FP resonator

$$I(\beta)=\frac{(1-R)^2\times e^{-2k\beta L}+4\times\sin^2(\psi)}{(1-R\times e^{-2k\beta L})^2+4R\times e^{-2k\beta L}\times\sin^2(\psi+n\beta L)} \tag{2}$$

and a spectral envelope, $E(\beta)$, defined by

$$E(\beta)=\frac{1}{1+\left[\frac{2\pi}{w}\times\left(\frac{1}{\beta_0}-\frac{1}{\beta}\right)\right]^2}. \tag{3}$$

$E(\beta)$ describes the Lorentz-shaped spectral envelope with a full width at half maximum of $2\pi/w$ around the central wave number β_0. Since the Fourier transform of a product of two functions (i.e., the FP transmission curve and the spectral envelope) is equal to the convolution of the two transformed functions, we calculate first the transform of the geometrical series for the transmitted amplitude given in Eq. (1). This results in

$$A(d)=(1-R\times e^{2i\psi})\times\sum_{m=0}^{\infty}\frac{R^m\times e^{2im\psi}}{2[kL\times(m+0.5)+i(\pi d-nmL)]}. \tag{4}$$

After performing an auto-convolution with the Fourier transform of its complex-conjugate, $A^*(d)$, we get the transform of the transmitted intensity,

$$I(d)=\left|1-R\times e^{-2i\psi}\right|^2\times\sum_{l=0}^{\infty}\sum_{m=0}^{\infty}\frac{R^{l+m}\times e^{-2i(l-m)\psi}}{kL\times(l+m+1)+i[\pi d+nL(l-m)]}. \tag{5}$$

Finally, the spectral envelope will be transformed as well and subsequently convolved with the transformed FP interferogram given by Eq. (5). Since this last mathematical operation involves tedious algebra, we state here as a general rule that a broad spectrum will yield narrow peaks in the transform and a narrow spectrum will give relatively broad peaks. The position of these peaks is given by $d=nL(l-m)/\pi$, where l and m are integers. We call the conjugate variable d of the wave number β optical path length. The variable d is proportional to the cavity length, and the proportionality factor is n/π. Although the complex function of Eq. (5) consists, in general, of amplitude and phase, we will use and plot the amplitude only for the following considerations. In addition, we will use units of μm for the optical path length.

Since, in Eq. (5), the facet reflectance and the cavity length are usually known, the only free parameter is the absorption coefficient k which is related to the cavity propagation loss/gain. One can therefore determine the cavity propagation loss/gain when performing a Fourier transform on a subthreshold emission spectrum. Obviously, the expansion into a geometrical series [Eq. (1)] fails for term ratios of unity or more, and we can use the method described above only below threshold.

In this work, we measured spectra of a red broad area laser at four different injection currents (120, 130, 140, and 150 mA) corresponding to 0.8, 0.867, 0.933, and $1\times I_{\mathrm{th}}$. A typical emission spectrum is shown in Fig. 1; it shows a FP mode spacing of 1.1 Å, corresponding to a 450 μm cavity length. This spectrum was obtained at an injection current of 140 mA ($0.933\times I_{\mathrm{th}}$). The numerical Fourier transform of this spectrum is shown as an inset of Fig. 1. There is a main peak at $d_0=450$ μm, corresponding to the cavity length, and several smaller peaks at integer multiples of d_0. The presence and the slow decay rate of these peaks indicate that the Q factor of the cavity is already high, and the shape of the individual FP modes is closer to a series of Dirac–delta functions than to a sine function. Moreover, when choosing a logarithmic scale for the y axis, there appears to be a unique ratio between the height of the adjacent peaks in the transform, i.e., the peaks of the harmonics lie on a straight line. Eventual deviations from this harmonic amplitude ratio (HAR) are due to the fact that we are averaging across a wavelength range over which gain/loss and therefore k do not remain constant. In Fig. 2, we show Fourier transforms of experimental data for three different current levels (120, 130, and 140 mA); the decreasing decay rate of the harmonic peaks at higher injection current levels is clearly visible.

Figure 3 shows the numerical Fourier transforms of analytically calculated emission spectra for the same current levels as in Fig. 2. The relative height of the peaks, their shape, and position agree very well with the experimental data. At 150 mA, which is very close to lasing threshold, only a fair agreement could be achieved, and the calculated cavity propagation gain value disagreed with the threshold condition

$$g_{\mathrm{th}}=\alpha+\frac{1}{L}\ln\frac{1}{\sqrt{R_1R_2}} \tag{6}$$

for lasing. This was because of the limited spectral resolution of the employed spectrometer. Since we can measure only

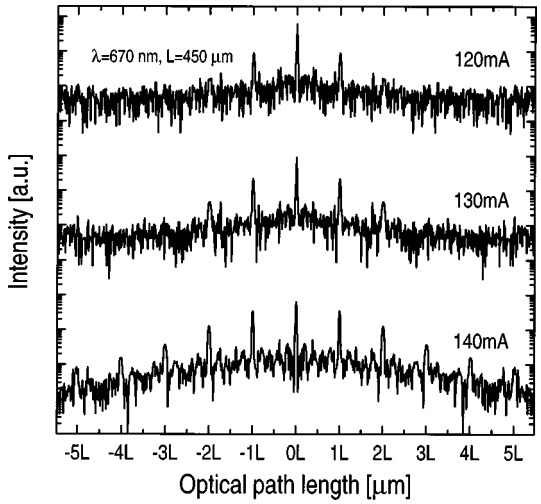

FIG. 2. Fourier transforms of experimental laser spectra at injection current levels of 120, 130, and 140 mA.

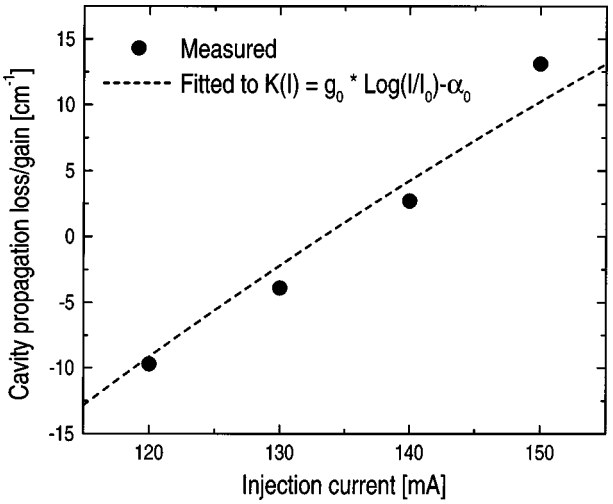

FIG. 4. Cavity propagation loss/gain vs injection current for a 450 μm long red broad area laser. The fitted line assumes a logarithmic gain/current behavior.

limited sharp peaks ($\Delta\lambda = 0.1$ Å), we cannot characterize cavities with Q factors beyond 10 for this particular wavelength. This explains the deviation of the experimental data from the calculation when coming close to threshold. For this particular device, the threshold current was roughly at 150 mA. The injection current at which the gain in the laser cavity equals the cavity propagation loss is the transparency current and this point could be easily detected at 135 mA. It is characterized by $g = \alpha$ in Eq. (6) or $k = 0$ in Eq. (5).

The HAR, r, in Fig. 2 is related to K, the cavity propagation loss/gain, via $r = R \times \exp(-KL)$. For the investigated injection current levels (120, 130, 140, and 150 mA), we determined HAR values of 0.20, 0.26, 0.35, and 0.56, and corresponding loss/gain values of -9.7, -3.9, 2.7, and 13.1 cm^{-1}, respectively. Since, with our current experimental setup, the HAR can be determined within $\pm 5\%$ only, our present measurements are limited to this precision. These values are represented by dots in Fig. 4. The dashed line is a fit of the curve $K(I) = g_0 \times \log(I/I_0) - \alpha_0$ through these points. The values we obtained when performing this fit were $\alpha_0 = 10$ cm^{-1}, $I_0 = 120$ mA, and $g_0 = 200$ cm^{-1}. The consistency of our cavity loss result with values obtained by other methods[10,11] is somewhat surprising given the lateral multimode behavior of our device. However, it shows that the cavity properties of the different filaments of a broad area laser resonator are sufficiently coherent that a well-defined, although broadened, series of harmonic peaks becomes apparent in the Fourier transform.

In conclusion, we have shown a new powerful method with which the optical gain of a laser cavity can be determined easily. The method is based on Fourier analysis of subthreshold laser spectra and measurement of the HAR in these Fourier transforms. The transparency current level can be determined as well as the total internal loss. Because of its easy implementation, this method might become useful for practical applications such as characterization and improvements of laser facet coatings or FP étalons.

The authors would like to thank Michael Kneissl for performing the spectral measurements on these samples, Decai Sun for processing assistance, and Fred Endicott for help in setting up the experiment.

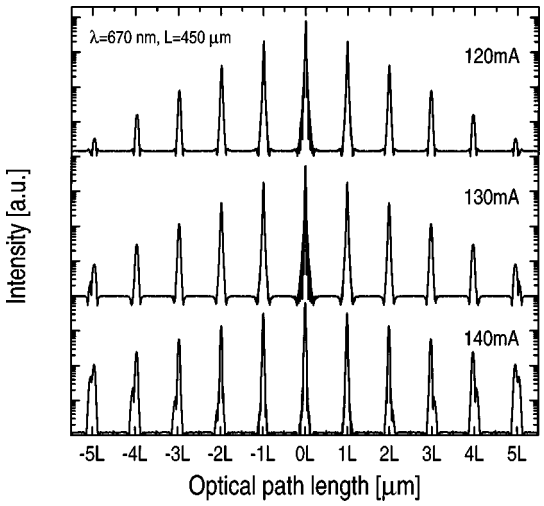

FIG. 3. Fourier transforms of simulated laser spectra. The cavity propagation loss/gain values have been chosen to match these data to the corresponding experimental data of Fig. 2.

[1] B. W. Hakki and T. L. Paoli, J. Appl. Phys. **44**, 4113 (1973).
[2] B. W. Hakki and T. L. Paoli, J. Appl. Phys. **46**, 1299 (1975).
[3] M. Born and E. Wolf, *Interference and Interferometers, Principles of Optics*, 6th ed. (Pergamon, New York, 1984), p. 256.
[4] B. D. Patterson, C. Musil, H. Siegwart, and A. Vonlanthen, Microelectron. Eng. **27**, 347 (1995).
[5] B. D. Patterson, Proc. Opt. Eng. **34**, 2289 (1995).
[6] V. G. Cooper, Appl. Opt. **10**, 525 (1971).
[7] D. M. Rust, Opt. Eng. (Bellingham) **33**, 3342 (1994).
[8] W. B. Cook, H. E. Snell, and P. B. Hays, Appl. Opt. **34**, 5263 (1995).
[9] D. P. Bour, T. L. Paoli, R. L. Thornton, D. W. Treat, Y. S. Park, and P. S. Zory, Appl. Phys. Lett. **62**, 3458 (1993).
[10] D. P. Bour, K. J. Beernink, D. W. Treat, T. L. Paoli, and R. L. Thornton, IEEE J. Quantum Electron. **30**, 2738 (1994).
[11] I. P. Kaminow, G. Eisenstein, and L. W. Stulz, IEEE J. Quantum Electron. **19**, 493 (1983).